Supporting Information

Spectral dependence of plasmon-enhanced fluorescence in a hollow nanotriangle assembled by DNA origami: towards plasmon assisted energy transfer

Petra Ivaskovic,[†,‡] Atsushi Yamada,[†] Juan Elezgaray,[‖] David Talaga,[‡] Sébastien Bonhommeau,[‡] Mireille Blanchard-Desce,[‡] Renaud A. L. Vallée[†] and Serge Ravaine*[†]*

[†] CNRS, Univ. Bordeaux, CRPP, UMR 5031, F-33600 Pessac, France.

[‡] CNRS, ISM, UMR 5255, Univ. Bordeaux, F-33400 Talence, France.

[‖] CNRS, CBMN, UMR 5248, Univ. Bordeaux, F-33607 Pessac, France.

Section 1. FDTD simulations

The simulation of plasmon propagation in the GNT with the anisotropic medium shown in Figure 1 and Figure S1 is performed by using our hand-made FDTD software in order to demonstrate a possibility of light path selectivity. The geometry of the structure (Figure 1 a) is composed of a hollow gold triangle with 60 nm external side length, 10 nm width of the side

and 15 nm thickness. The gold triangle is placed on a flat glass substrate and the hollow is filled by an anisotropic medium with molecular polarization orientation of 45 degree with respect to the x-direction in the xy plane. This anisotropic part is described by the dielectric tensor

$$\boldsymbol{\varepsilon} = \varepsilon_0 \begin{bmatrix} 1 & & \\ & 1 & \\ & & 1 \end{bmatrix} + \varepsilon_0 \mathbf{U}(\theta) \begin{bmatrix} \varepsilon_{\parallel} - 1 & & \\ & \varepsilon_{\perp} - 1 & \\ & & \varepsilon_{\perp} - 1 \end{bmatrix} \mathbf{U}(\theta)^{-1}, \qquad \text{(S1)}$$

where ε_0, $\varepsilon_{\parallel}$, and $\varepsilon_{\perp}$ are the dielectric constants in vacuum and along parallel and perpendicular directions of molecules, respectively. **U**(θ) represents a rotation matrix allowing for the tuning of the angle θ (tuning of molecular orientation). The second term of the right-hand side of Eq. (S1) thus fixes the polarizations along the parallel and perpendicular directions of the molecules in the xy plane. In the calculation, $\varepsilon_{\parallel}$ is set as 4 while no polarization was assumed in the perpendicular direction for simplicity, i.e. $\varepsilon_{\perp}$=1. The system shown in Figure1a is structured with a grid size of 1.25 nm, where absorbing boundary conditions are set in all directions. The time step was determined by a courant factor of 0.5. The incident light source is represented by a Gaussian point source in space, placed at 7.5 nm from the left gold corner. The pulse (in time) is a cosine function with a wavelength of 780nm modulated by a Gaussian envelope and polarized along the x-direction (that is, x-component of the electric field). A snapshot of the electric field intensity shown in Figure 1b and the movie in Figure S1 clearly exhibit the path selectivity, where the strongest intensity has been found at the right-bottom corner of the GNT.

FigureS1. Movie exhibiting the path selectivity in a hollow GNT filled by an anisotropic medium with molecular polarization orientation of 45 degree with respect to the x-direction in the xy plane.

The optical properties of the investigated round-triangle deposited on a glass substrate were analyzed using a three-dimensional finite-difference time-domain software (FDTD Solutions, from Lumerical Solutions, Inc.) The geometry of the structure consists in a hollow (equilateral) gold triangle with a 64 nm (28 nm) external (internal) side length and a 16 nm thickness (Figure 4 a)). In order to closely mimic the experimental structure, the triangle has been rounded with a corner's radius of 12 nm, in agreement with the measurements performed by AFM (Figure 2 c)). The rounded triangle is then deposited flat on a glass substrate. The dielectric properties of the various components are a dispersion-less dielectric permittivity of 2.151 for glass, together with the permittivity of gold from the software database as described by Palik[1] (0-2 μm). The simulation space was constructed using perfectly matched layers (PMLs) along all axes. The excitation of the structure was performed by using a broadband 2.66 fs pulse centred at 541 THz, with a bandwidth of 416 THz, launched along the vertical z-axis and polarized along x (Figure 4 a)). Owing to the implementation of a Total Field Scattered Field formulation, the absorption, scattering and extinction cross-sections of the whole structure were obtained in one step (Figure 4 b)). In a second step, the electric field amplitude profile was obtained for the two dominant resonance modes of interest (633 and 690 nm). The mode corresponding to 633 nm, which corresponds to the experimental excitation wavelength, is shown in the inset of Figure 4 b), allowing one to estimate the excitation enhancement. Finally, in order to compute the emission rate enhancement of the emitters located at the corners of the nano-structure (Figure 4 c)), we performed Fourier transforms of the response to an impulsive point-dipole polarized radially to the structure, 6 nm away from it, in order to obtain a maximum effect. We then normalized this response with the one obtained for a point-dipole source located in vacuum under the same excitation conditions.

Section 2. Experimental

Silver nitrate (99,9%, Aldrich), trisodium citrate dehydrate (Aldrich), sodium borohydride (≥98%, Aldrich), ascorbic acid (Aldrich), polyvinylpyrrolidone (Mw~ 55 000, Aldrich), sodium polystyrene sulfonate (Aldrich), hydroxylamine hydrochloride (99.995%, Aldrich), sodium hydroxide (Aldrich), hydrogen tetrachloroaurate III (99.995%, Aldrich), ascorbic acid (Aldrich), hydrogen peroxide solution (30 % (w/w) in water, Aldrich), acetic acid (≥99.5%, Aldrich), Ethylenediaminetetraacetic acid (EDTA, ≥99%, Aldrich), magnesium acetate tetrahydrate (≥99%, Aldrich), ammonium hydroxide solution (Aldrich) were used as received. All ssDNA staples were purchased from Eurogentec (France) and kept as 100 µM aqueous stock solutions. mPEG-thiol (Mw= 5000) was bought from JenKem Technology.

TEM experiments were performed with a Hitachi H600 microscope operating at 75 kV. The samples were prepared as follows: colloidal dispersions were diluted in ethanol and one drop was deposited on a copper grid coated with a carbon membrane and left to evaporate. AFM height images were realized in soft tapping mode by means of commercial silicon AFM cantilevers (Nanosensors, PPP-NCST, nominal resonance frequency 160 kHz, nominal force constant 7.4 N/m). UV-visible spectra were recorded using a Perkin-Elmer Lambda 950 spectrophotometer. Colocalized AFM and fluorescence measurements were carried out using an instrument described in detail elsewhere[2].

1. **Synthesis of silver nanoprisms**

• Preparation of Ag seeds

In a standard experiment, ultrapure water (47.5 mL), trisodium citrate solution (0.5 mL, 30 mM) and $AgNO_3$ solution (1 mL, 5 mM) were introduced in a 100 mL two-necked round bottom flask immersed in an ice-bath. The mixture was bubbled with argon under stirring during 30 min to remove oxygen. The argon flow was transferred at the surface of the solution and cold, freshly prepared aqueous solution of $NaBH_4$ (0.5 mL, 50 mM) was rapidly injected

in the mixture under vigorous stirring. The reaction was allowed to proceed during 16 min during which 4 drops of the prepared $NaBH_4$ solution were added every 2 minutes to ensure complete reduction of silver ions. Finally, a mixture of a polystyrene sulfonate solution (0.5 mL, 5 mg/mL) with the prepared $NaBH_4$ solution (0.25 mL) was added drop-wise to the yellow reaction mixture. The solution was stirred at room temperature under argon flow during 4 h to complete decomposition of the remaining borohydride ions.

During the Ag seeds synthesis, the addition of $NaBH_4$ caused the immediate color change of a clear solution to yellow which intensified as the seeds aged for 5h, indicating the formation of Ag nanoparticles. The seed diameter was estimated to 4 ± 2 nm by the statistical analysis of TEM images (Figure S2). The absorbance spectra showed a band at 384 nm, consistent with the expected plasmon resonance of Ag nanoparticles with this size (Figure S2).

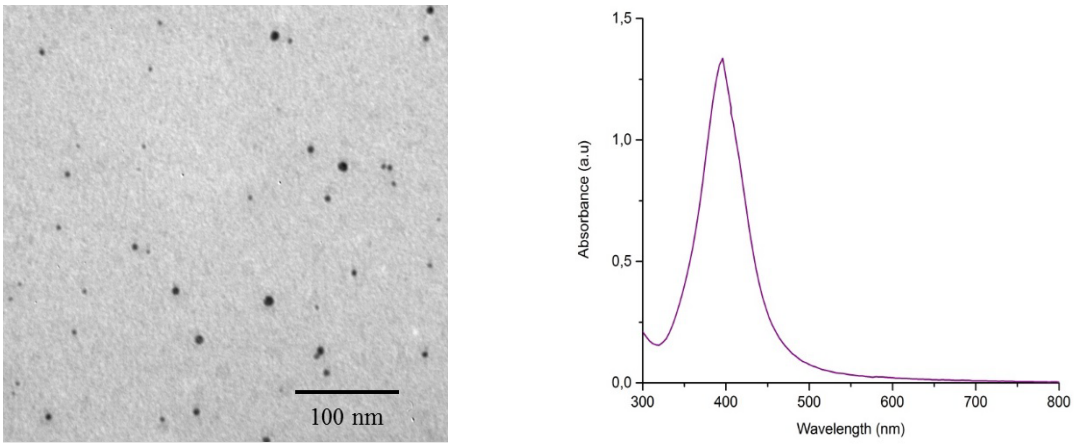

Figure S2. Left: TEM image of the Ag seeds. Right: Absorbance spectrum of the Ag seeds in water.

• Seeded growth of the nanoprisms

Prepared silver seeds (3.5 mL) were added to the mixture of ultrapure water (100 mL), ascorbic acid solution (100 mL, 0.5 mM), trisodium citrate solution (38 mL, 30 mM), and polyvinylpyrrolidone solution (PVP, Mw~ 55 000, 38 mL, 0.7 mM). An $AgNO_3$ solution (12.5 mL, 2.5 mM) was introduced in the mixture with a syringe pump. The addition rate was

set to 10 mL/h. The reaction was performed at room temperature, under vigorous stirring, protected from light exposure. The color of the solution progressively changed from yellow to orange, pink, purple, and finally deep blue.

The addition of the seeds in the growth solution containing ascorbic acid, citrate and PVP was followed by the introduction of the silver precursor. Owing to their large surface area, the seeds served as a substrate for the decomposition of ascorbic acid which was used to reduce the Ag^+ ions and cause their deposition on the Ag nuclei. The seeds can grow in circular, hexagonal or triangular plates, depending on the reaction kinetics and the ratio of the growth rates of {111} and {100} facets of the seeds. If the reduction rate is very fast, the number of atoms supplied from the bulk is too large for the seeds to incorporate them, resulting in the formation of spherical particles. Thus, to promote the growth of triangular nanoparticles, a moderate reduction rate is required. Citrate was shown to have a crucial role in the decrease of the reaction kinetics. As it adsorbs on the seed surface, a negatively charged monolayer is formed on the surface, delaying the penetration of the ascorbate anions and the citrate-silver complexes to the seed surface. Consequently the rate of silver reduction is slowed down, leading to the smooth nanoprism formation. Another key parameter for the nanoprism formation is the growth ratio between {111} and {100} facets of Ag seeds. Both capping agents adsorb onto the growing seed and thus alter the kinetics of the relative growth rates. The protonation state of the citrate ions can be adjusted to favor the growth rate in the {111} direction, leading to smooth nanoprism formation[3]. The obtained silver nanoparticles were characterized by TEM. Figure S3 shows that they mainly have the target triangular morphology, even though they coexist with some spherical nanoparticles. The average edge length and thickness of the silver nanoprisms were estimated to be 45 ± 8 nm and 8 ± 1 nm, respectively. The absorption spectrum of the nanoprisms shows four characteristic surface plasmon bands (Figure S3), indicating the formation of thin and flat nanocrystals. The first three weak signals centered at 340 nm, 400 nm and 456 nm correspond to out-of-plane

quadrupole, out-of-plane dipole and in-plane quadrupole plasmon resonances, respectively. The strong absorption peak at 616 nm is attributed to the in-plane dipole resonance mode and it highly depends on the nanoprism length, thickness and tip truncation.[4]

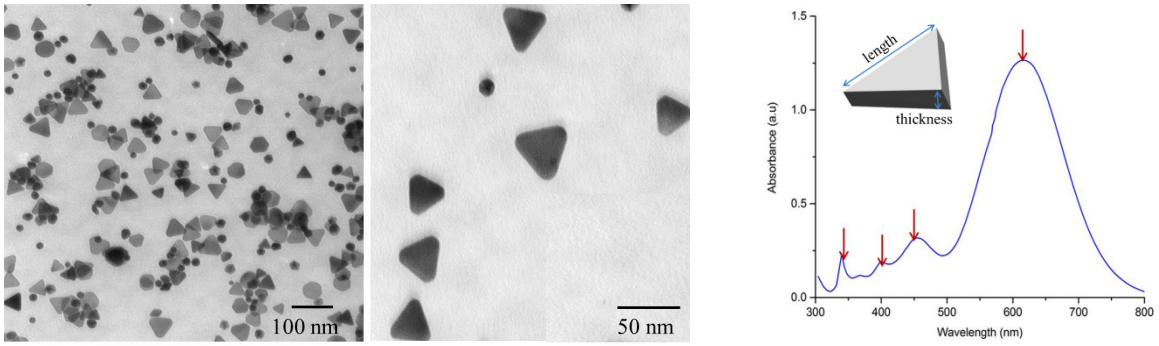

Figure S3. Left and middle: Low and high magnification TEM images of the Ag nanoprisms. Right: Absorbance spectrum of the Ag nanoprisms in water.

2. Synthesis of Au-framed Ag nanoprisms

A gold layer was successfully deposited on the edges of the Ag nanoprisms following a protocol adapted from the paper published by Shahjamali *et al.*[5] Each individual Ag nanoprism contains two main {111} facets on the triangular planes and three {100} facets on the edges. Since the {100} facets have a higher surface energy than that of the {111} ones, the gold atom deposition preferentially takes place at the prism edges.[6] The epitaxial growth of the gold layer is favored by the lattice mismatch between gold and silver (<0.3 %). While the Au@Ag core-shell nanostructures can be easily synthesized, the formation of the reverse structures with Ag core and Au shell is limited by the galvanic replacement process. It is an electrochemical process which involves oxidation of one metal by the ions of another more noble metal. However, such process has limited capability to achieve monometallic hollow nanostructures with precise control over morphology. As it involves simultaneous oxidative etching of the template and the atom deposition of the more noble metal onto the template, it leads to the formation of semi-hollow nanostructures with many pinholes (Figure S4 left).

Therefore, a mild reducing agent, hydroxylamine hydrochloride (HyA), was used to deposit the gold on the sides of the nanoprism.[5] However, the selective deposition is not guaranteed if the gold concentration is not carefully tuned. Any excess of gold above the critical Ag/Au ratio can lead to Ag etching by galvanic replacement, following the equation:

$3Ag\ (s) + AuCl_4^-\ (aq) \rightarrow Au\ (s) + 3\ Ag^+\ (aq) + 4\ Cl^-\ (aq)$

Therefore, in a typical experiment, the as-prepared silver nanoprism solution (20 mL) was centrifuged (10 000 rpm, 40 min) and redispersed in ultrapure water (20 mL). Hydroxylamine hydrochloride (HyA) solution (3 mM) and $HAuCl_4$ solution (0.3 mM) were then added simultaneously via two separate syringe pumps. The addition rate was set to 2 mL/h. After 5 min of addition, original HyA solution was replaced with basic HyA solution for additional 15 min of addition. Basic HyA solution was prepared by mixing original HyA solution (15 mL, 3 mM) and sodium hydroxide solution (0.30 mL, 0.5 M). The reducing power of HyA is enhanced at higher pH values, so NaOH was introduced to increase pH and boost the gold deposition rate. Ag@Au nanoprisms solution was then centrifuged (12 000 rpm, 45 min) and redispersed in an aqueous solution of trisodium citrate (15 mL, 0.3 mM).

We performed a set of experiments to find the highest concentration of gold salt which results in the nanoprism edge coating but without pinhole formation. We observed that for the given volume of synthesized Ag nanoprisms, 0.67 mL of $HAuCl_4$ solution is the optimal amount. This concentration was shown to be too low to induce the etching but high enough to ensure the deposition of Au atoms on the {100} facets of the Ag nanoprism, as the high surface energy of these facets enables effective activation of the reaction between HyA and $HAuCl_4$. The chemical reactions involved in the gold coating process are the following:

$6\ NH_3OH^+ \leftrightarrow 6e^- + 12H^+ + 6\ H_2O + 3N_2$

$2\ Au^{3+} + 4\ e^- \rightarrow 2\ Au^+$

$2\ Au^+ + 2\ e^- \rightarrow 2\ Au^0$

At this stage of the synthesis, Au-framed Ag nanoprisms were obtained, as shown in Figure S4. One can see nanostructures with darker edges as a consequence of the higher electron density of gold by comparison with silver. The gold coating process was also monitored by UV-vis spectroscopy, revealing a red shift and a decrease of the intensity of the LSPR band with time (Figure S4 right). This spectral change is assigned to the gold deposition on the Ag prism edges, as gold has a higher refractive index than silver in the visible range.

With the increase of the volume of $HAuCl_4$ solution above 0.67 mL, the {111} facets of the silver nanoprisms start to be etched through galvanic corrosion, but the Ag nanoprism edges stay protected by the initially deposited Au layers. The oxidation of Ag nanoprisms by gold ions occurs due to the difference in the redox potentials between Ag^+/Ag (0.8 V vs. SHE; SHE = standard hydrogen electrode) and $AuCl_4^-/Au$ (0.99 V vs. SHE). The galvanic oxidation of the silver nanoprisms results in the formation of triangular nanostructures with many pinholes (Figure S4 middle).

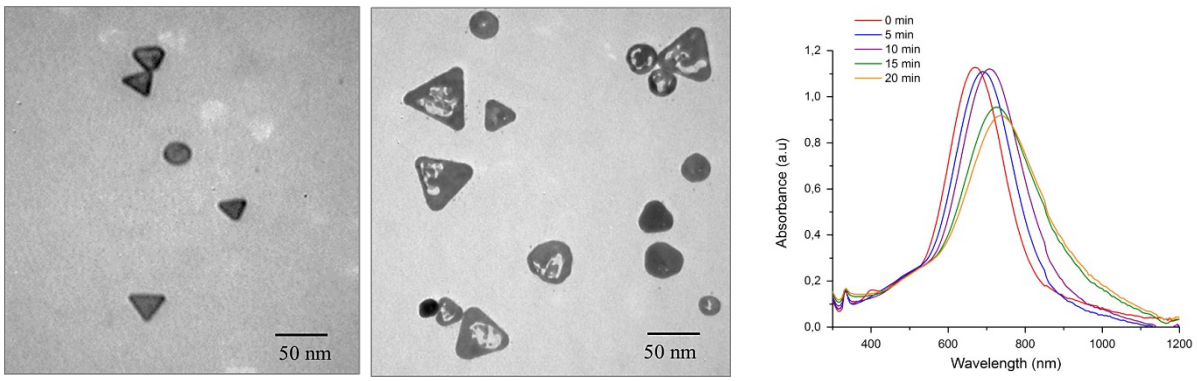

Figure S4. TEM images of Au-framed Ag nanoprisms obtained by the addition of the optimal amount (left) and an excess of the gold salt (middle). Right: Temporal evolution of the UV-visible spectra of the silver nanoprisms during the gold deposition onto their edges.

3. Synthesis of gold hollow nanotriangles

The etching of the Ag nanoprism template was carried out through a treatment with a mixture of hydrogen peroxide and ammonium hydroxide, as reported by Shahjamali *et al.*[6] Briefly,

hydrogen peroxide (50 mM) and ammonium hydroxide (50 mM) were mixed in 1:1 volume ratio and the mixture (0.8 mL) was introduced by a syringe pump (addition rate: 3 mL/h) to a freshly prepared solution of Au-framed Ag nanoprisms (4 mL). The mixture was then centrifuged (9 000 rpm, 30 min) and the gold triangular nanoframes were redispersed in an aqueous solution of trisodium citrate (4 mL, 0.3 mM).

In such mixture, H_2O_2 oxidizes Ag atoms according to:

$$Ag\,(s) + 1/2H_2O_2\,(aq) \rightarrow Ag^+\,(aq) + OH^-\,(aq)$$

while NH_4OH acts as a coordination agent to dissolve the oxidized silver following the reaction:

$$Ag^+\,(aq) + 2NH_4OH\,(aq) \rightarrow [Ag(NH_3)_2]^+\,(aq) + 2H_2O$$

and prevents the formation of AgOH or Ag_2O that may precipitate onto the prisms and hamper further etching reaction.[7] Such mixture behaves like a mild wet etchant as it induces the etching of Ag without contaminating the particles with ligands or ions. The TEM image shown in Figure S5 revealed that upon the etching process, the silver template was removed from the Au-framed Ag nanoprisms, leading to hollow GNTs with a mean size of 60 nm.

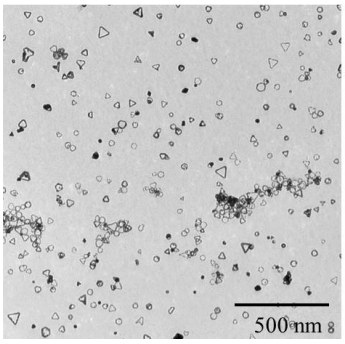

Figure S5. TEM image of the hollow GNTs.

4. Synthesis of a DNA origami modified with thiols and fluorescent dyes

DNA origami assembly was done by mixing scaffold (ssDNA isolated from bacteriophage M13mp18) and staples to a final concentration of 10 nM and 50 nM, respectively, in a TAE buffer that contained 40 mM Tris, 20 mM acetic acid, 1 mM EDTA and 10 mM magnesium

acetate. The mixture was then subjected to thermal annealing. The temperature was first raised to 90 °C, then decreased to 60 °C during 1 h, and finally decreased to 20 °C during 2 h. The assembled origami structures were purified from the excess staple strands by centrifugation with 100 kDa MWCO filters and collected at the end of the second cycle of centrifugation. An AFM image of the rectangular DNA origami structures is shown in Figure S6.

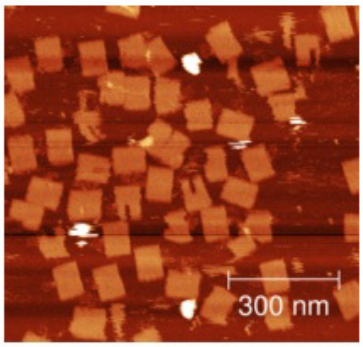

Figure S6. Peak force topographical AFM image of the rectangular DNA origami structures.

5. Stabilization of gold hollow nanotriangles in TAE buffer

10 µL of an aqueous stock solution of mPEG-thiol (M_n= 5000 g mol^{-1}; 6.5 mg/mL) were added to a solution of the freshly prepared hollow GNTs solution (4 mL, 6.5 10^{11} particles). The mixture was stirred for 2h and then washed with water by two centrifugation cycles (7 500 rpm, 20 min), to remove free mPEG-SH. After the second centrifugation, the supernatant was discarded and PEG-coated hollow nanotriangles were redispersed in a TAE buffer which contained magnesium cations ([Mg^{2+}] = 10 mM). The PEG-coated hollow GNTs were stable in TAE buffer during at least few weeks (Figure S7).

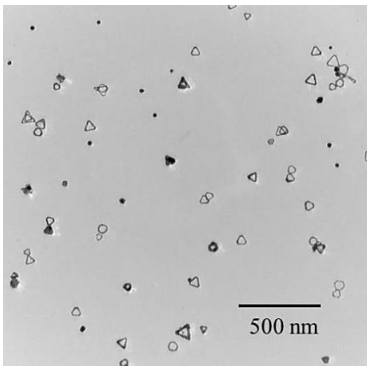

Figure S7. TEM image of PEG-capped hollow GNTs in TAE buffer.

(1) Palik, E. D. *Handbook of Optical Constants of Solids*, Academic, San Diego, 1985.

(2) Vilar-Vidal, N.; Bonhommeau, S.; Talaga, D.; Ravaine, S. *New J. Chem.* **2016**, 40, 7299-7302.

(3) Le Beulze, A.; Duguet, E.; Mornet, S.; Majimel, J.; Tréguer-Delapierre, M.; Ravaine, S.; Florea, I.; Ersen, O.New insights into the side-face structure, growth aspects, and reactivity of Ag_n nanoprisms. *Langmuir* **2014**, 30, 1424–1434.

(4) Jin, R.; Cao, Y. C.; Hao, E.; Métraux, G. S.; Schatz, G. C.; Mirkin, C. A. Controlling anisotropic nanoparticle growth through plasmon excitation. *Nature* **2003**, 425, 487–490.

(5) Shahjamali, M. M.; Bosman, M.; Cao, S.; Huang, X.; Saadat, S.; Martinsson, E.; Aili, D.; Tay, Y. Y.; Liedberg, B.; Loo, S. C. J.; Zhang, H.; Boey, F.; Xue, C. Gold coating of silver nanoprisms. *Adv. Funct. Mater.* **2012**, 22, 849–854.

(6) Shahjamali, M. M.; Salvador, M.; Bosman, M.; Ginger, D. S.; Xue, C. Edge-gold-coated silver nanoprisms: Enhanced stability and applications in organic photovoltaics and chemical sensing. *J. Phys. Chem. C* **2014**, 118, 12459–12468.

(7) Shahjamali, M. M.; Bosman, M.; Cao, S.; Huang, X.; Cao, X.; Zhang, H.; Pramana, S. S.; Xue, C. Surfactant-free sub-2 nm ultrathin triangular gold nanoframes. *Small* **2013**, 9, 2880–2886.